eLIFE
elifesciences.org

Figures and figure supplements

Requirement for highly efficient pre-mRNA splicing during *Drosophila* early embryonic development

Leonardo Gastón Guilgur, et al.

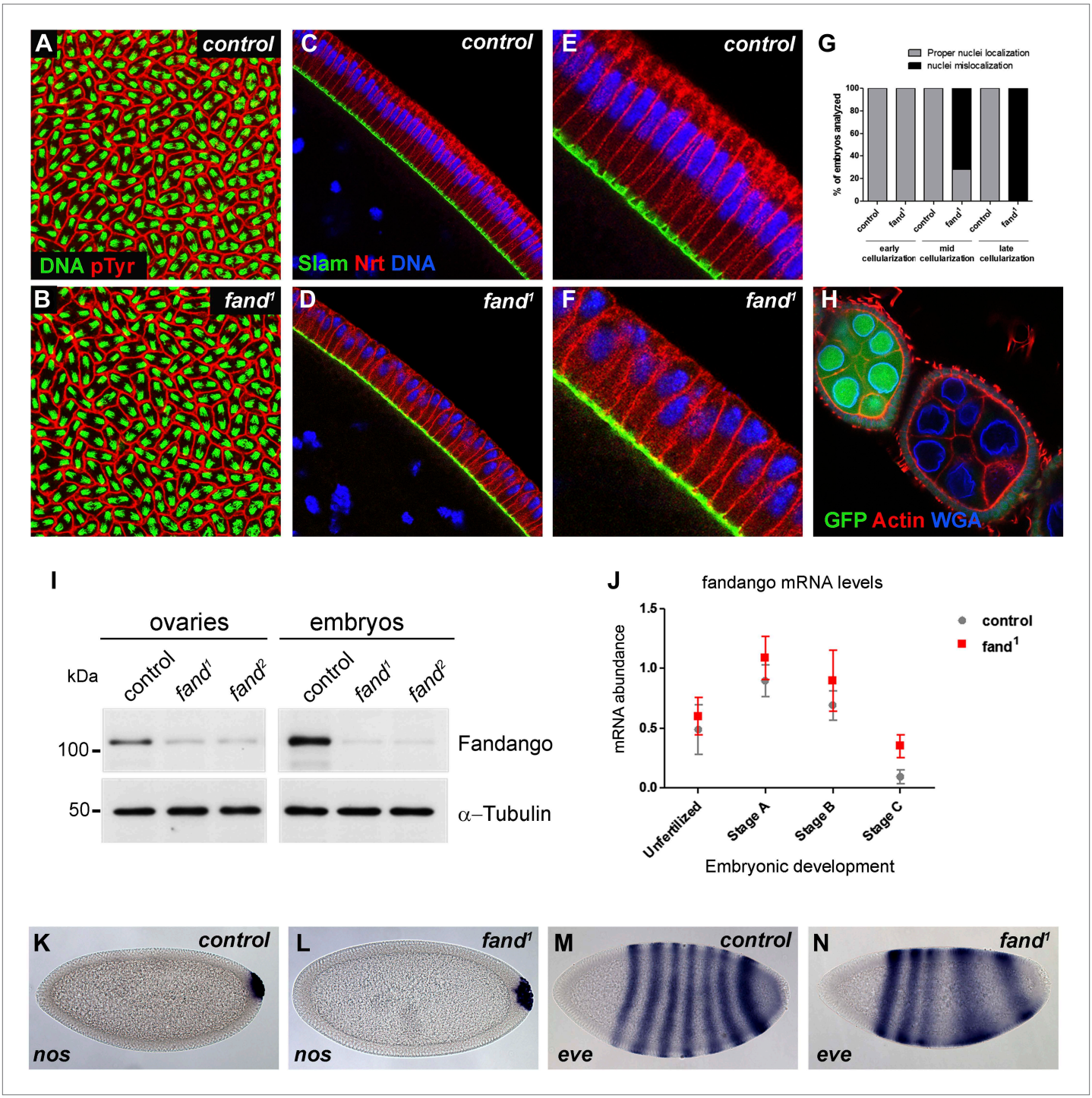

Figure 1. Drosophila Fandango/Xab2 is required for blastoderm cellularization. (**A** and **B**) Panels show embryos with normal syncytial blastoderm nuclear divisions in control embryos (*hs*-FLP; FRT42B) (**A**) and *fand*^{1} germ-line clone embryos (*hs*-FLP; FRT42B *fand*^{1}, maternal mutant) (**B**). Embryos were stained for DNA (green) and p-Tyrosine (red). (**C**–**F**) Panels show blastoderm cellularized embryos. Control embryos showed normal epithelial architecture with elongated nuclei and columnar cell shape (**C**). *fand*^{1} germ-line clone mutant embryos showed abnormal epithelial architecture, the cortical nuclei failed to elongate and became mislocalized (**D**). (**E** and **F**) Magnification of **C** and **D,** respectively. Embryos were stained for Slam (green), Neurotactin (red), and DNA (blue). (**G**) Quantification of *fandango* maternal mutant embryo phenotype during blastoderm cellularization. Early cellularization: control: 100% normal (n = 44), *fand*^{1}: 100% normal (n = 49); mid cellularization: control: 100% normal (n = 25), *fand*^{1}: 28% normal (n = 21); late cellularization: control: 100% normal (n = 42), *fand*^{1}: 0% normal (n = 38). (**H**) Maternally controlled oogenesis was normal in *fandango* mutant clones. Absence of endogenous nGFP (green) indicated that the cells were homozygous for *fand*^{1} mutation. Ovaries were stained for F-actin (red) and WGA (blue). (**I**) Western blot of

Figure 1. Continued on next page

Figure 1. Continued

whole protein extracts from embryos and ovaries mutant for *fand*^{1} and *fand*^{2} alleles (germ-line clones) showed a clear reduction in Fandango protein levels compared to control tissues. It should be noticed that due to experimental constraints the total protein extracts from mutant ovaries included not only signal from mutant germ-line cells (homozygous for *fand*^{1}), but also the tightly associated heterozygote somatic follicle cells. α-Tubulin was used as a loading control. (**J**) Real-time qPCR analysis showed no significant differences in fandango mRNA levels between control and *fand*^{1} embryos during development (Two-way ANOVA p>0.05 ns.). fandango mRNA levels were normalized with β-actin mRNA levels. (**K**–**N**) in situ hybridization for *nanos* RNA (maternal) and *even-skipped* RNA (early zygotic) in blastoderm cellularized embryos. Both control (**K**) and *fand*^{1} mutant (**L**) embryos showed normal *nos* localization pattern in the pole cells. *fand*^{1} embryos (**N**) showed A–P patterning defects of *eve* compared to control embryos (**M**).

DOI: 10.7554/eLife.02181.003

A

Cross		Offspring					
		CyO flies			CyO^{+} flies (*w; fand*^{1}*/fand*^{2})		
	F1 ♂	n	%	% exp	n	%	% exp
♀ w/w; *fand*^{1}/CyO x ♂ *wt-fandango* ; *fand*^{2}/CyO		382	37	33	0	0	17
		CyO flies			CyO^{+} flies (w/*wt-fandango* ; *fand*^{1}/*fand*^{2})		
	F1 ♀	n	%	% exp	n	%	% exp
		448	43	33	187	18	17

Cross		Offspring					
		CyO flies			CyO^{+} flies (*wt-fandango* ; *fand*^{1}*/fand*^{2})		
	F1 ♂	n	%	% exp	n	%	% exp
♀ *wt-fandango* ; *fand*^{2}/CyO x ♂ *w/w* ; *fand*^{1}/CyO		176	33	33	82	15	17
		CyO flies			CyO^{+} flies (w/*wt-fandango* ; *fand*^{1}/*fand*^{2})		
	F1 ♀	n	%	% exp	n	%	% exp
		182	34	33	93	17	17

B Fandango/XAB2

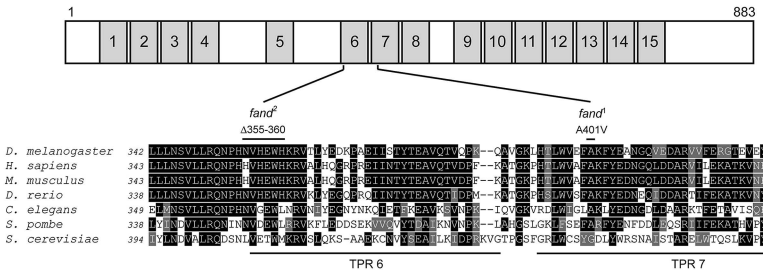

Figure 1—figure supplement 1. *fandango* mutant alleles contain changes in highly conserved amino acids.

DOI: 10.7554/eLife.02181.004

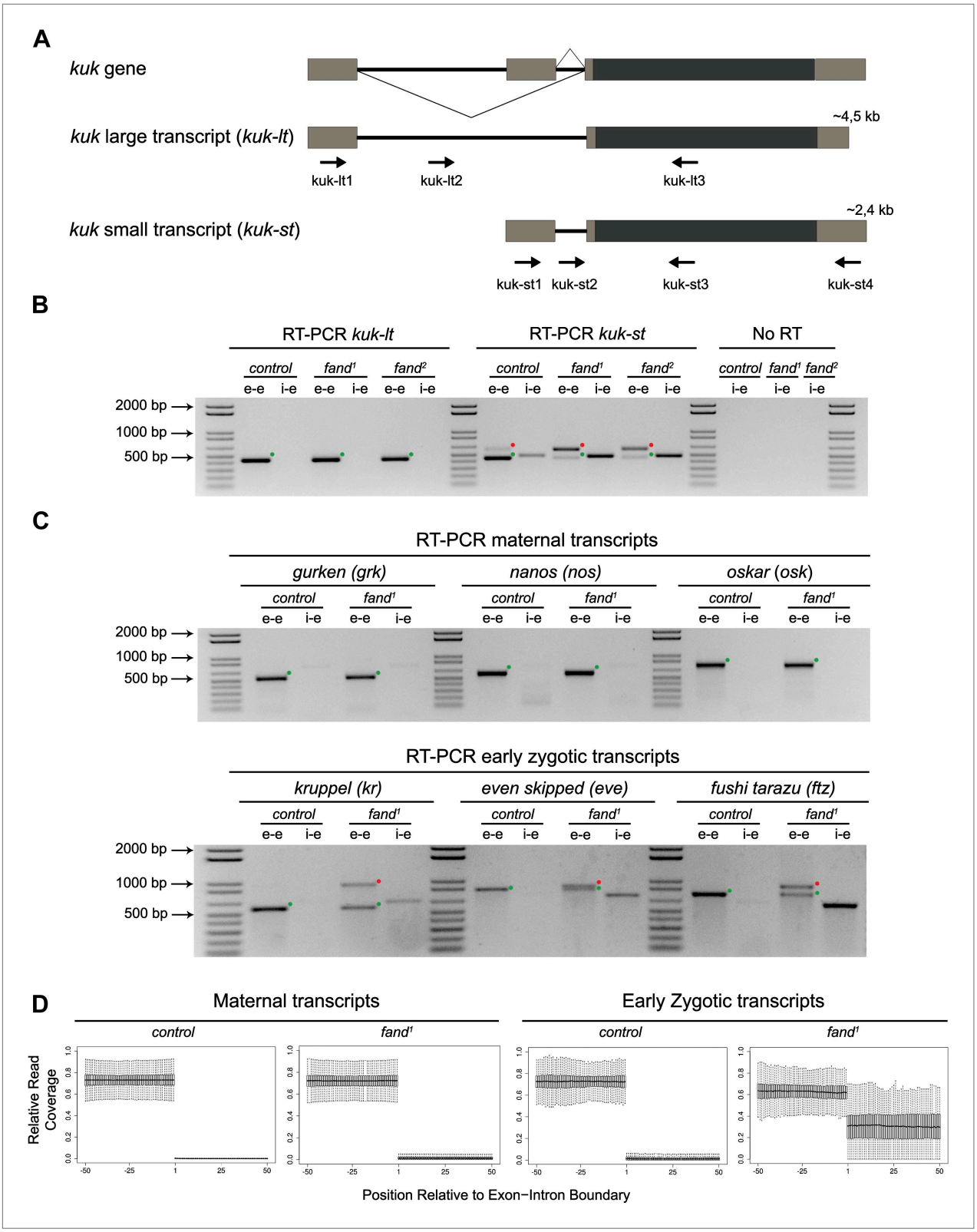

Figure 2. Splicing of early zygotic but not maternally encoded pre-mRNAs is affected in *fandango* mutants. (**A**) The *kugelkern* (*kuk*) locus encodes two transcripts of different size, *kuk-lt* containing a large intron and *kuk-st* with a short intron. Orientation and position of primers used for splicing analysis is indicated (arrows). (**B**) RT-PCR analysis of *kuk* transcripts. Control embryos yielded PCR products in the size predicted for the properly spliced forms of both *kuk* transcripts using exon–exon (e–e) primers (green dots, *kuk-lt*: 431 bp and *kuk-st*: 437 bp). *fandango* maternal mutant embryos

Figure 2. Continued on next page

Figure 2. Continued

(*fand*^{1} and *fand*^{2} alleles) showed splicing defects only in the *kuk-st* transcript; PCR products were detected by e–e primers in the size expected for intron retention (red dots, *kuk-st*: 596 bp) and by intron–exon (i–e) primers (*kuk-st*: 474 bp). Splicing of the *kuk-lt* was not affected in *fandango* mutant background; PCR products were only detected with e–e primers in the predicted size for the correctly spliced pre-mRNA (green dots, *kuk-lt*: 431 bp). 'No RT' controls (only total RNA as template) yielded no amplification, meaning there was no contamination with genomic DNA in the samples tested. (**C**) RT-PCR analysis of maternal and early zygotic genes. Maternal transcripts were properly spliced, in both, control and *fand*^{1} mutant embryos; PCR products were only detected using e–e primers (green dots, *grk*: 527, *nos*: 581, *osk*: 762 bp). In contrast, early zygotic transcripts were correctly spliced only in control embryos (green dots, *kr*: 559, *eve*: 828, *ftz*: 753 bp). *fand*^{1} mutant embryos yielded PCR products in the size predicted for intron retention with e–e primers (red dots, *kr*: 932, *eve*: 899, *ftz*: 900 bp) and with i–e primers (*kr*: 629, *eve*: 720, *ftz*: 595 bp). All PCR bands showed in the panels were cloned and sequenced to confirm their identity. Green dots indicate correctly spliced transcripts, red dots indicate unspliced transcripts (intron retention). (**D**) RNA-Seq data confirmed that zygotic but not maternally encoded transcripts displayed a large fraction of splicing defects (intron retention) in *fand*^{1} mutant embryos. The panel shows box plot of the distribution of numbers of reads per bp relative to the total number of reads falling inside a 100 bp window centered around the 5′splice sites of zygotic (n = 408 splice sites from 270 genes) or maternal genes (n = 5876 splice sites from 2048 genes).

DOI: 10.7554/eLife.02181.005

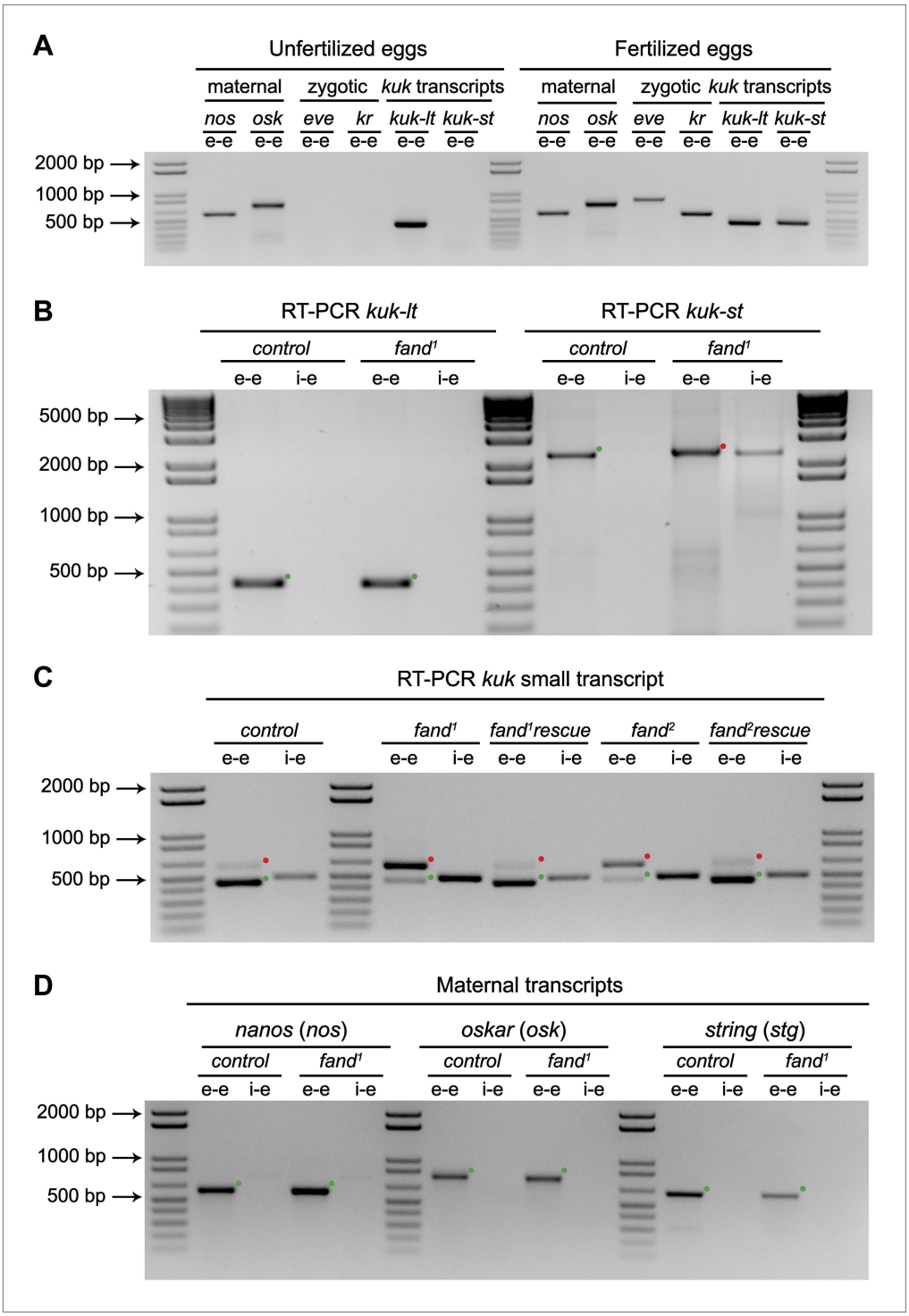

Figure 2—figure supplement 1. Splicing of early zygotic but not maternally encoded pre-mRNAs is affected in *fandango* mutants.

DOI: 10.7554/eLife.02181.006

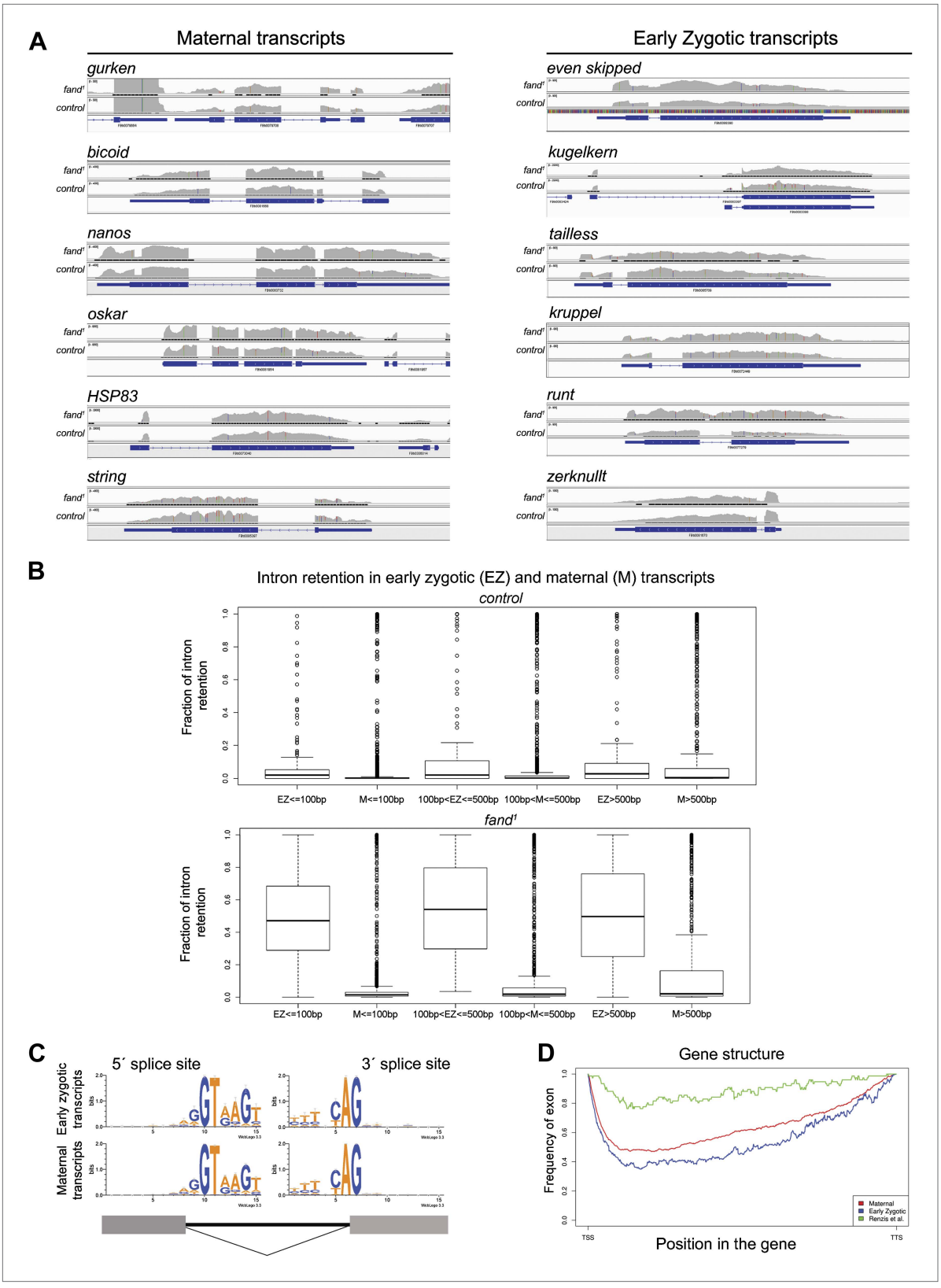

Figure 2—figure supplement 2. Early zygotic but not maternally encoded pre-mRNAs shows significant intron retention in *fandango* mutants.
DOI: 10.7554/eLife.02181.007

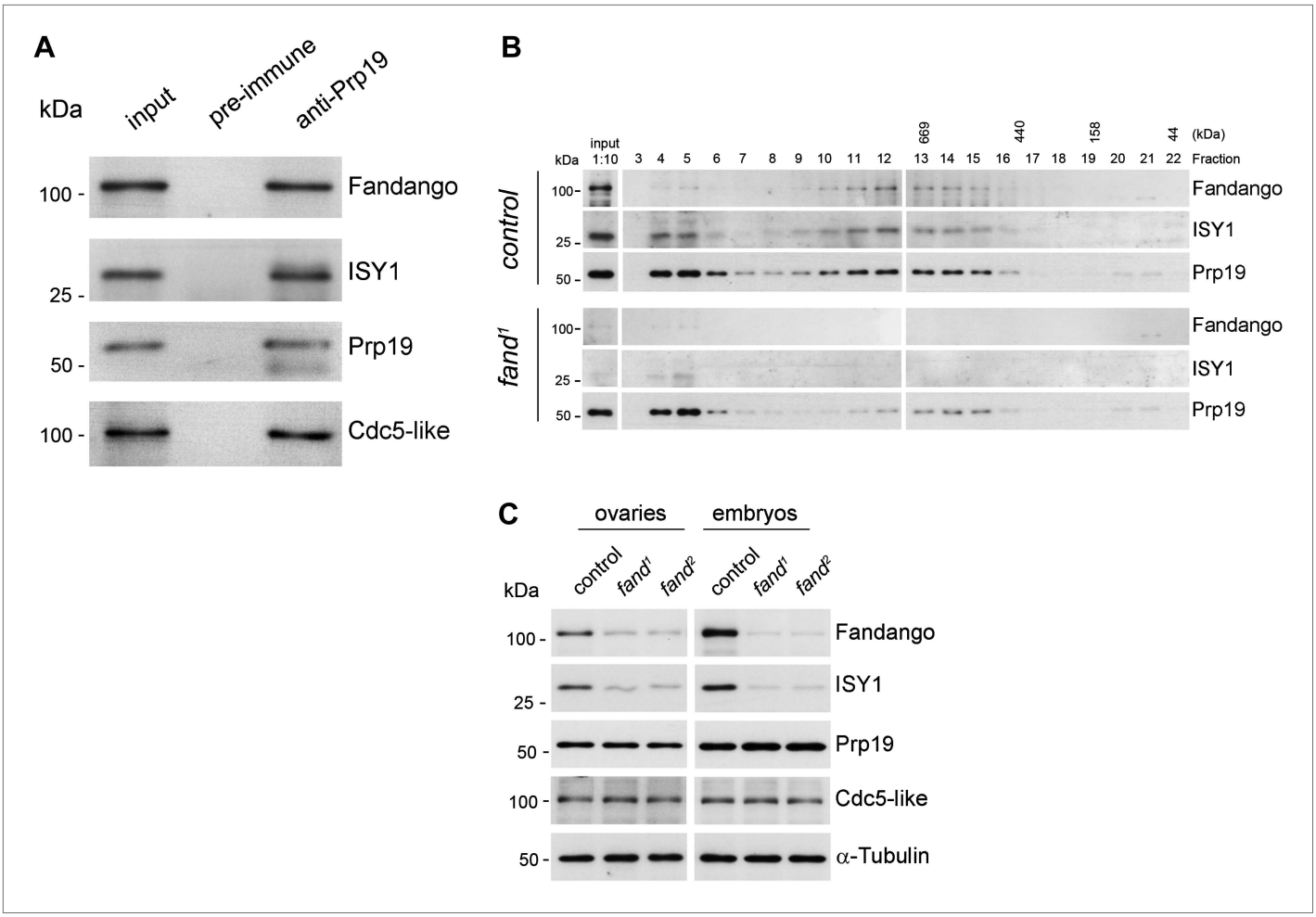

Figure 3. Fandango physically interacts with a similar group of splicing proteins during oogenesis and embryogenesis. (**A**) Pull down assay from nuclear-enriched protein extracts using a polyclonal antibody of Prp19. Endogenous Prp19 interacts physically with Fandango and other subunits of the NTC/Prp19 complexes (ISY1 and CDC5L). Pre-immune serum was used in the control. (**B**) Size-exclusion chromatography of control and *fand*^{1} mutant protein extracts from 0–3 hr embryo collections using a Superose 6 10/300 column. After separation, each fraction was analyzed by Western blot. NTC/Prp19 complexes subunits (Prp19, Fandango, and ISY1) were part of a ~600–800 kDa complex and also co-purified in a significantly larger complex (fraction 4 and 5). *fand*^{1} mutant protein extracts showed a significant reduction in levels of Fandango and ISY1 subunits and a size reduction of the Prp19-positive ~600–800 kDa complex. (**C**) Western-blot analysis of total protein extracts from ovaries (left) and 0–3 hr embryos (right) from control and both *fandango* alleles, showed a reduction of Fandango and ISY1 protein levels in both tissues. Protein levels of Prp19 and CDC5L were not affected. α-Tubulin was used as loading control. Fandango Western blot is the same as shown in ***Figure 1I***.

DOI: 10.7554/eLife.02181.008

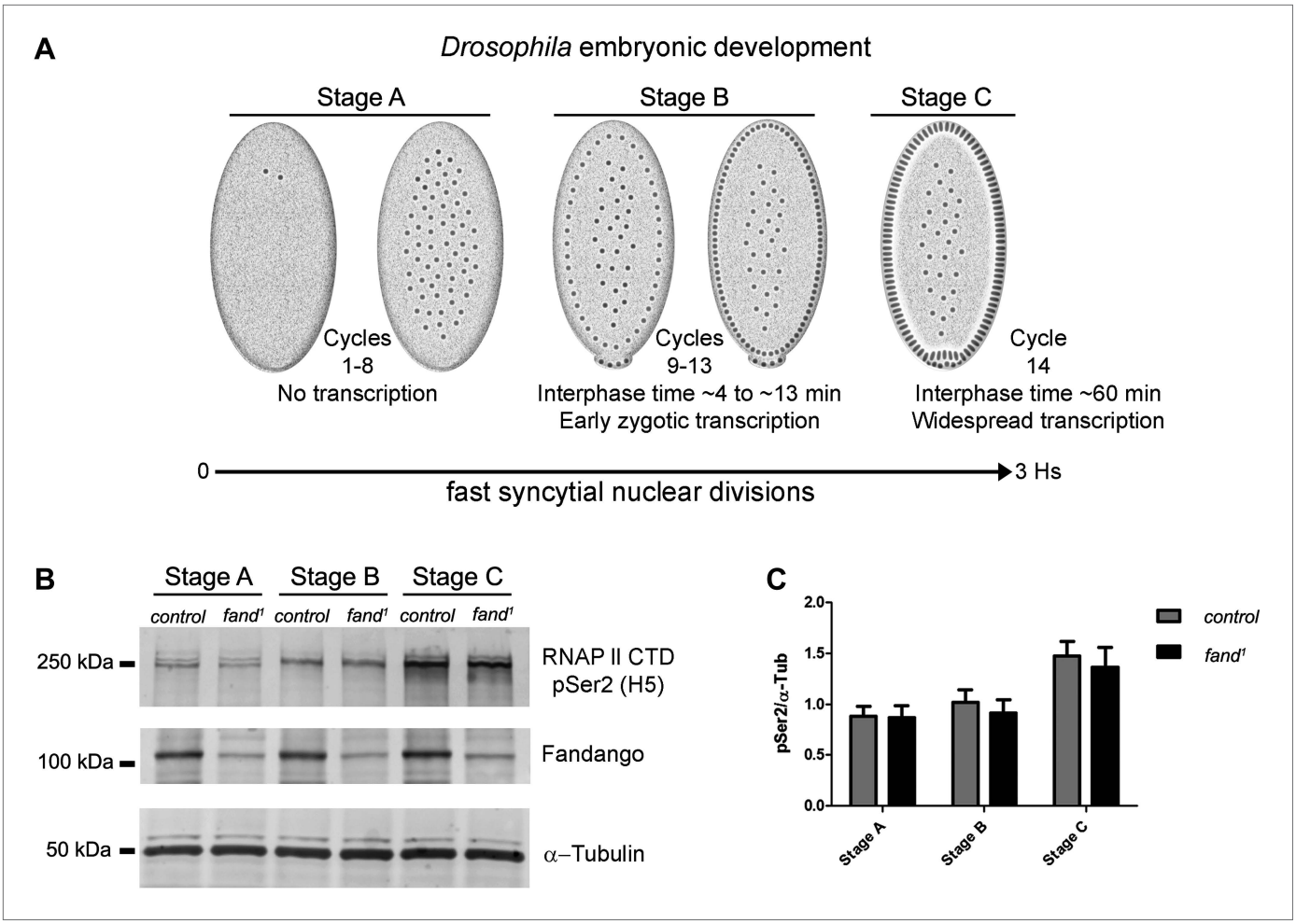

Figure 4. Early zygotic transcription is not affected during mid/late-syncytial blastoderm in *fandango* mutants. (**A**) Embryos were divided into three different groups according to developmental stage ('Materials and methods'), stage A: early/mid-syncytial blastoderm embryos, stage B: mid/late-syncytial blastoderm embryos, and stage C: blastoderm cellularization embryos. (**B**) Western blot for RNApol II CTD Ser2 phosphorylation levels. Control and *fand*^{1} embryos showed a similar increase in the global levels of RNApol II CTD Ser2 phosphorylation over the course of early embryonic development. α-Tubulin was used as a loading control. (**C**) Quantification of the CTD Ser2 phosphorylation from five independent western blot assays showed no significant difference at any of the embryonic developmental stages analyzed (Two-way ANOVA p>0.05 ns.).

DOI: 10.7554/eLife.02181.010

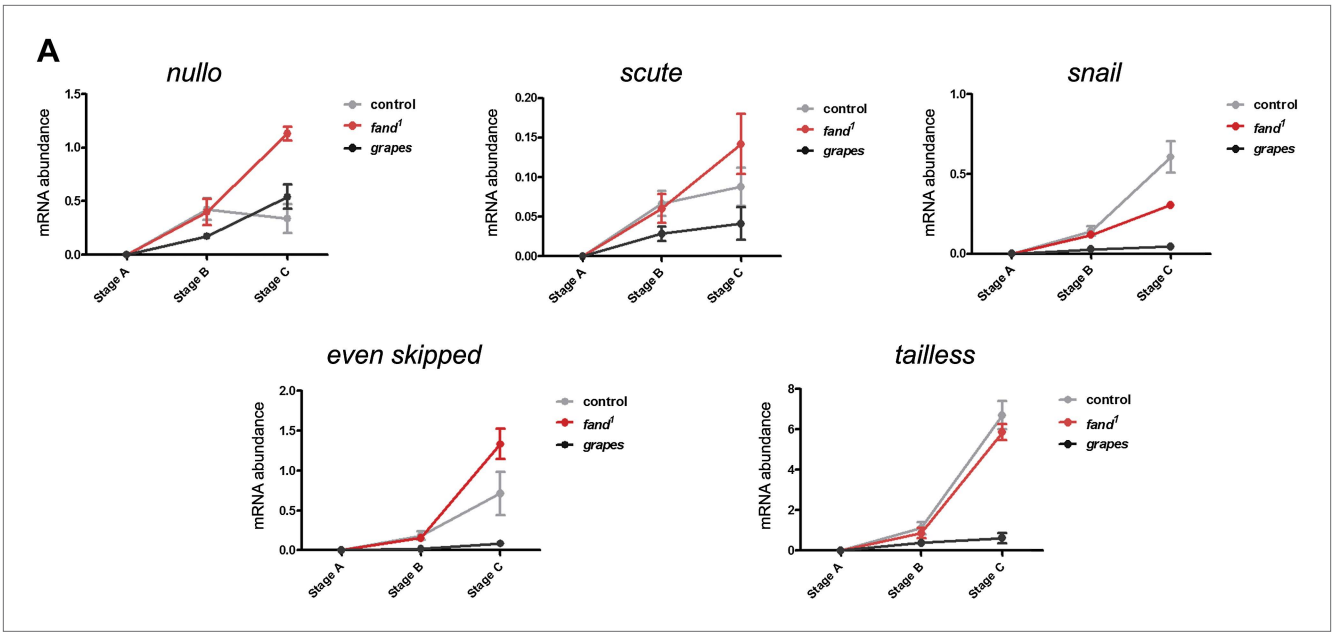

Figure 4—figure supplement 1. Early zygotic transcription is not affected during mid/late-syncytial blastoderm in *fandango* mutants.
DOI: 10.7554/eLife.02181.011

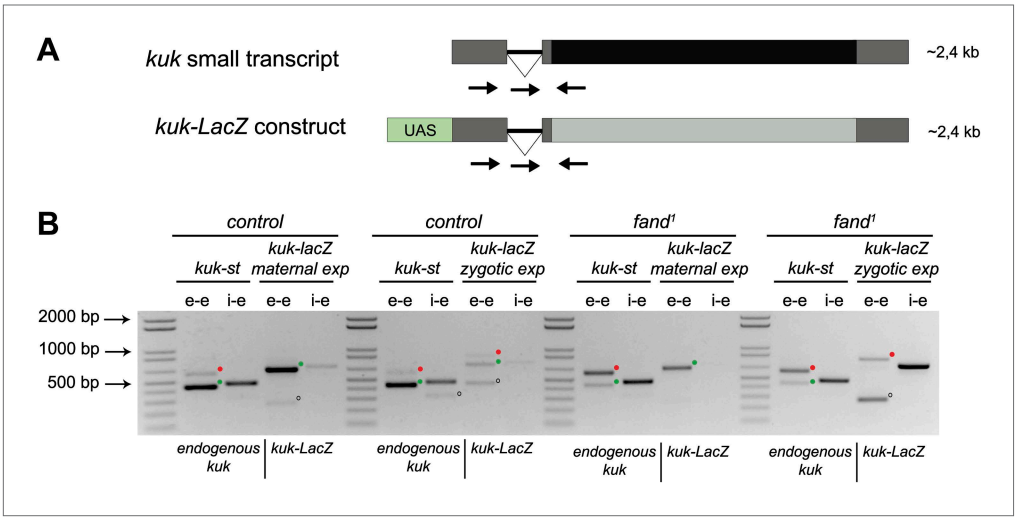

Figure 5. Ectopic maternal expression of an early zygotic transcript in the mutant background is sufficient to suppress its splicing defects. (**A**) The *kuk-LacZ* construct was built using the 5′UTR, the intron and the 3′UTR of the *kuk* small transcript (dark gray), and replacing the *kuk* ORF (black) by the LacZ coding sequence (light gray). To induce the expression of this construct it was put under the control of the UAS promoter (green) to drive the tissue specific expression with GAL4 drivers. Orientation and position of primers used for splicing analysis is indicated (arrows). (**B**) RT-PCR analysis of the *kuk-LacZ* construct. When it was zygotically expressed, it was correctly spliced in control but not in *fand*[1] embryos (similarly to the endogenous small *kuk* transcript). Intron retention with e–e primers (red dots, *kuk-st*: 596 bp and *kuk-LacZ*: 869 bp) and a PCR product with i–e primers (751 bp) were observed in the mutant. When it was maternally expressed, *kuk-LacZ* construct was correctly spliced both in control and *fand*[1] embryos, being detected just the spliced form of the construct (green dots, *kuk-st*: 437 bp and *kuk-LacZ*: 713 bp). In contrast, the endogenous zygotically expressed small *kuk* transcript (*kuk-st*) is still poorly spliced in *fand*[1] embryos carrying the *kuk-LacZ* construct. Open circles indicate unspecific PCR products (confirmed by sequencing). Green dots indicate correctly spliced transcripts, whereas red dots indicate unspliced transcripts (intron retention).
DOI: 10.7554/eLife.02181.012

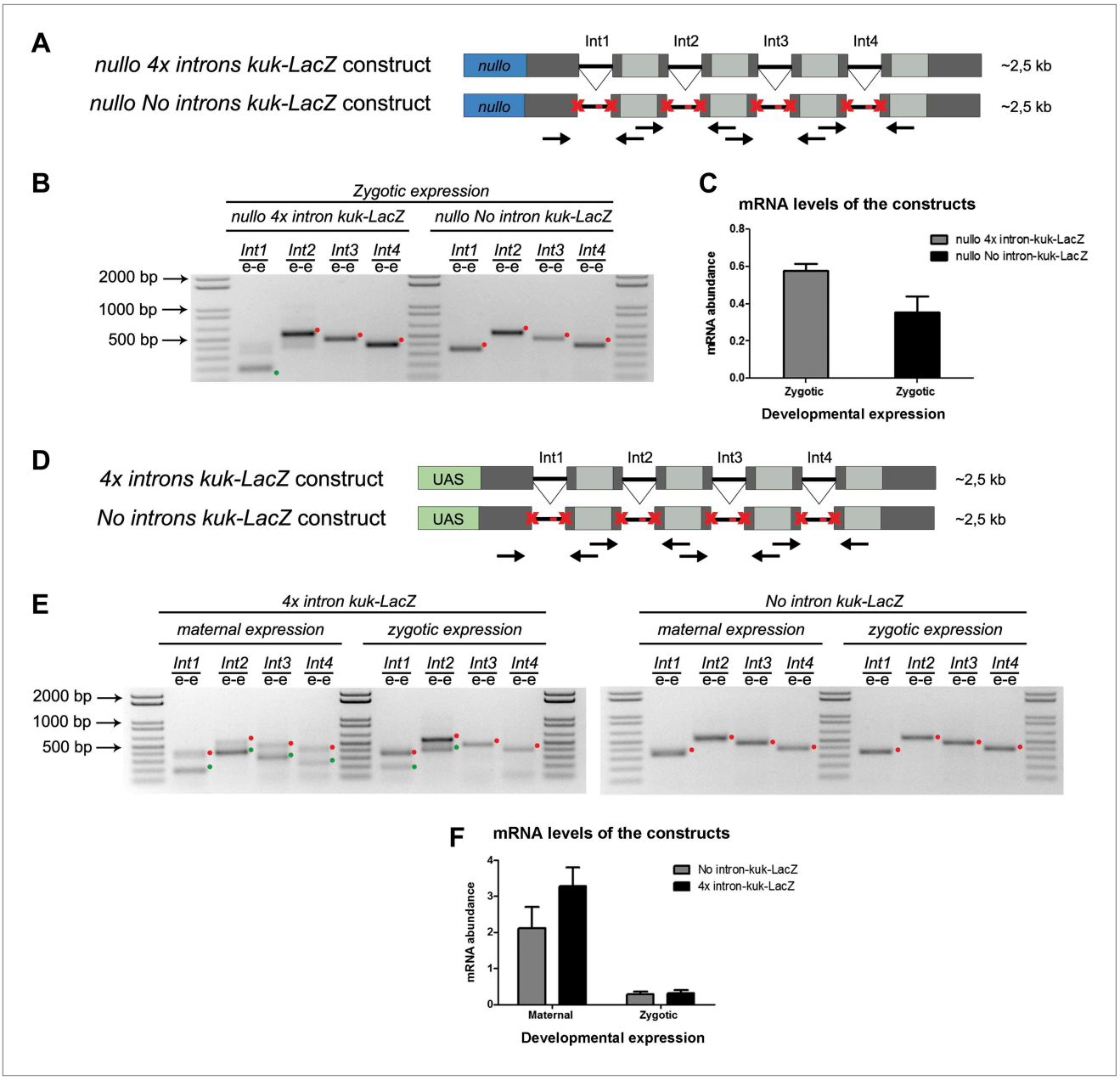

Figure 6. A small early zygotic transcript containing four introns is poorly spliced in wild-type embryos. (**A** and **D**) The *4x intron kuk-LacZ* construct was a variant of the *kuk-LacZ* that contains four copies of *kuk* small transcript intron (dark gray). Each intron is separated by 201 nucleotides of an in frame Lac-Z sequence (light gray). The *no intron kuk-LacZ* construct has all splice sites present in the *4x intron kuk-LacZ* construct mutated to thymidines. The constructs were fused to a *nullo* minimal promoter (blue) (**A**), or fused to an inducible UAS promoter (green) (**D**). Orientation and position of primers used for splicing analysis is indicated (arrows). (**B**) RT-PCR analysis showed significant splicing defects (intron retention) of the *4x intron kuk-LacZ* construct when expressed under the control of an endogenous early zygotic promoter (*nullo* promoter). The first intron was correctly spliced, being detected mainly the PCR product corresponding to the spliced form (green dot). The remaining introns (second, third, and fourth) were completely unspliced (red dots, intron retention). In the intronless (*no intron kuk-LacZ*) construct, under the control of the same *nullo* promoter were only observed PCR bands whose sizes correspond to unspliced forms (red dots, intron retention). (**C**) Real-time qPCR analysis showed that the *4x intron kuk-LacZ* and *no intron kuk-LacZ* constructs were expressed to the same extent when under the control of the *nullo* minimal promoter (*t* test p>0.05 ns.). (**E**) RT-PCR analysis of the *4x intron kuk-LacZ* construct showed significant splicing defects (intron retention) when zygotically expressed in wild-type embryos under the control of an inducible UAS promoter. Although the most 5′-localized introns (first and second) were still partially spliced, being observed two PCR bands corresponding to the spliced (green dots, int1: 191 and int2: 385 bp), and unspliced forms (red dots, int1: 347 and int2: 541 bp). The furthest 3′-localized introns (third and fourth) were completely unspliced, being only observed one PCR band with the size corresponding to intron retention (red dots, int3: 463 and int4: 385 bp). Maternal expression of the *4x intron kuk-LacZ* construct was sufficient to significantly suppress splicing defects in

Figure 6. Continued on next page

Figure 6. Continued

the four introns analyzed (green dots, spliced forms: int1: 191, int2: 385, int3: 307, int4: 229 bp; red dots, unspliced forms: int1: 347, int2: 541, int3: 463, int4: 385 bp). Zygotic and maternal expression of the *no intron kuk-LacZ* construct only showed PCR bands with sizes corresponding to unspliced forms (red dots, intron retention). (**F**) Real-time qPCR analysis showed that the *4x intron kuk-LacZ* and *no intron kuk-LacZ* constructs were expressed to the same extent both maternally (Two-way ANOVA $p>0.05$ ns.) and zygotically ($p>0.05$ ns.) in wild-type embryos. All PCR bands shown in these panels were cloned and sequenced to confirm their identity. Green dots indicate correctly spliced transcripts, red dots indicate unspliced transcripts (intron retention).

DOI: 10.7554/eLife.02181.013